A Greener Synthesis of Core (Fe, Cu)−Shell (Au, Pt, Pd, and Ag) Nanocrystals Using Aqueous Vitamin C

ARTICLE *in* CRYSTAL GROWTH & DESIGN · NOVEMBER 2007

Impact Factor: 4.89 · DOI: 10.1021/cg070554e

2 AUTHORS:

Mallikarjuna N. Nadagouda
United States Environmental Protection A…
164 PUBLICATIONS **3,965** CITATIONS
SEE PROFILE

Rajender S Varma
United States Environmental Protection A…
541 PUBLICATIONS **15,514** CITATIONS
SEE PROFILE

CRYSTAL GROWTH & DESIGN
2007
VOL. 7, NO. 12
2582–2587

A Greener Synthesis of Core (Fe, Cu)-Shell (Au, Pt, Pd, and Ag) Nanocrystals Using Aqueous Vitamin C

Mallikarjuna N. Nadagouda and Rajender S. Varma*

Sustainable Technology Division, United States Environmental Protection Agency, National Risk Management Research Laboratory, 26 West Martin Luther King Drive, MS 443, Cincinnati, Ohio 45268

Received June 18, 2007; Revised Manuscript Received September 10, 2007

ABSTRACT: A greener method to fabricate novel core (Fe and Cu)-shell (noble metals) metal nanocrystals using aqueous ascorbic acid (vitamin C) is described. Transition metal salts such as Cu and Fe were reduced using ascorbic acid, a benign naturally available antioxidant, and then addition of noble metal salts resulted in the formation of the core–shell structure depending on the core and shell material used for the preparation. Pt yielded a tennis ball kind of structure with a Cu core, whereas Pd and Au formed regular spherical nanoparticles. Au, Pt, and Pd formed cube-shaped structures with Fe as the core. Inversely, transition metals with noble metals, such as Pd, as the core also formed interesting structures; these structures were brushlike with indium as the shell and needle-like when Cu was employed as the shell. The method is general uses no surfactant or capping agent and can be extended to noble metals as cores and transition metals as shells. The core–shell nanocrystals were characterized using transmission electron microscopy (TEM), selected area electron diffraction (SAED), and UV–vis spectroscopy. These nanocrystals have unique properties that are not originally present in either the core or shell materials and may have potential functions in catalysis, biosensors, energy storage systems, nanodevices, and ever-expanding other technological applications.

Introduction

Considerable efforts have been devoted to bimetallic nanoparticles owing to their different catalytic properties,[1–3] surface plasma band energy,[4,5] and magnetic properties[6,7] relative to the individual metals. A number of methods have been used to prepare the bimetallic nanoparticles, including alcohol reduction,[1,8,9] citrate reduction,[5,10] polyol processes,[11] borohydride reduction,[12] solvent extraction– reduction,[4,13,14] sonochemical methods,[15] photolytic reduction,[16,17] radiolytic reduction,[18,19] laser ablation,[20,21] and biological programming.[22]

However, materials that are derived from core–shell particles are of extensive scientific and technological interest, due to their unique and tailored properties for various applications in materials science.[23–27] Recently, efforts to prepare core–shell particles have been focused on the composite particle with a metallic nanoshell. Metal-coated colloidal core–shell composite particles have their potential uses as catalysts, sensors, substrates for surface-enhanced Raman scattering (SERS), and colloidal entities with unique optical properties.[28–30] Narayan et al. have reported that with proper manipulation of the Au shell in the core–shell nanoparticles, SERS hot spots can be produced. They further showed the difference in SERS properties of core–shell nanoparticles with and without the hot spots and their utility to detect various biomolecules at nanomolar concentrations without the use of Raman markers as reported earlier.[31,32] Jang et al. showed that gold nanorods can be coated with thickness-controlled silver by reducing $AgCl_4$ exclusively on the metallic surface to form Au-core Ag-shell nanorods and then restored by selectively removing the silver coating; such nanorods show much sharper, stronger, and shorter-wavelength surface plasmon absorption than gold nanorods.[33] Many routes have been explored to fabricate such core–shell particles, such as using poly(ethylene amine),[34] electroless plating,[35] surface precipitation reaction,[36] laser pulses,[37] and self-assembly.[25] However, in most cases, the degree of surface coverage is low, and the metallic coating is nonuniform, owing to the interparticles coulomb repulsion and/or the passivation of metallic nanoparticles caused by a capping agent.[38] Therefore, to prepare a composite particle with a uniform and complete coverage of metallic nanoshell remains a challenge, and newer techniques need to be explored and evaluated for their application in the preparation of interesting optical materials. Recently, we accomplished a shape-selective synthesis of noble nanoparticles and nanowires using vitamin B_2 without using any harmful reducing agents, such as sodium borohydride ($NaBH_4$) or hydroxylamine hydrochloride, or surfactants.[39] Vitamin B_2 was used as reducing agent as well as a capping agent due to its high water solubility, biodegradability, and low toxicity compared with other reducing agents. In continuation of our efforts to develop novel greener methods to synthesize noble nanostructures,[40,41]

Table 1. Core–shell Compositions Tested During Study

entry	composition
1	2 mL $CuCl_2$ + 10 mL ascorbic acid + 2 mL $HAuCl_4 \cdot 3H_2O$
2	2 mL $CuCl_2$ + 10 mL ascorbic acid + 2 mL $Na_2PtCl_6 \cdot 6H_2O$
3	2 mL $CuCl_2$ + 10 mL ascorbic acid + 2 mL $PdCl_2$
5	2 mL $Fe(NO_3)_3 \cdot 9H_2O$ + 10 mL ascorbic acid + 2 mL $PdCl_2$
6	2 mL $Fe(NO_3)_3 \cdot 9H_2O$ + 10 mL ascorbic acid + 2 mL $HAuCl_4 \cdot 3H_2O$
7	2 mL $Fe(NO_3)_3 \cdot 9H_2O$ + 10 mL ascorbic acid + 2 mL $Na_2PtCl_6 \cdot 6H_2O$
8	2 mL $Fe(NO_3)_3 \cdot 9H_2O$ + 10 mL ascorbic acid + 2 mL $Na_2PtCl_6 \cdot 6H_2O$
9	5 mL $PdCl_2$ + 2 mL ascorbic acid + 5 mL $HAuCl_4 \cdot 3H_2O$
10	5 mL $PdCl_2$ + 2 mL ascorbic acid + 5 mL $Na_2PtCl_6 \cdot 6H_2O$
11	5 mL $PdCl_2$ + 2 mL ascorbic acid + 5 mL $InCl_3$
12	5 mL $PdCl_2$ + 2 mL ascorbic acid + 5 mL $Fe(NO_3)_3 \cdot 9H_2O$
13	5 mL $PdCl_2$ + 2 mL ascorbic acid + 5 mL $CuCl_2$

Scheme 1. Schematic Diagram of Formation of the Pt-Cu Core–Shell Nanostructures

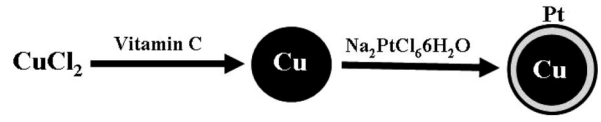

* To whom correspondence should be addressed. Tel: (513) 487-2701. Fax: (513) 569-7677. E-mail: varma.rajender@epa.gov.

10.1021/cg070554e CCC: $37.00
Published on Web 11/09/2007

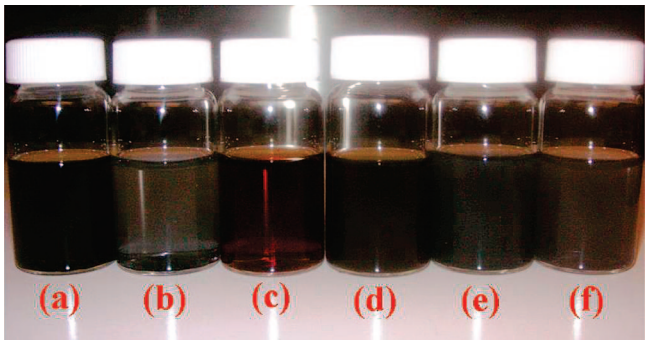

Figure 1. Photographic images of ascorbic acid reduced bimetallic nanostructures of (a) Fe-Pd, (b) Au-Pt, (c) Pt-Fe, (d) Au-Fe, (e) Pd-Pt, and (f) Au-Pd nanocrystals.

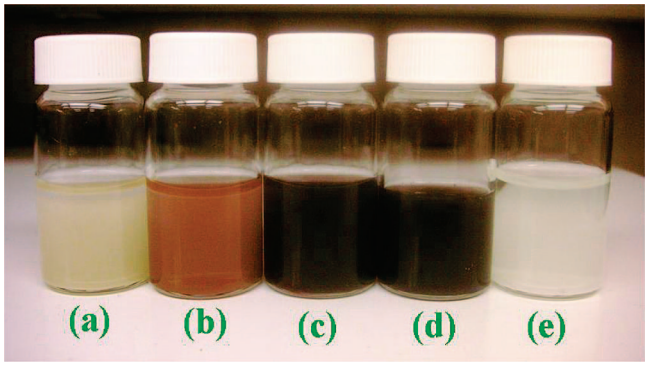

Figure 2. Photographic images of ascorbic acid reduced metallic nanostructures of (a) Ag, (b) Au, (c) Pd, (d) Pt, and (e) Cu nanocrystals.

herein we report an environmentally benign approach that provides facile entry to production of multiple shaped core–shell particles, where noble metals such as Au, Pd, Ag, and Pt nanoparticles tethered on Cu and or Fe served as nucleation sites for the growth of a noble metal nanoshell overlayer.

Experimental Procedures

All chemical reagents used in this study were of analytical grade and used without any further purification. The reactants used were $Na_2PtCl_6 \cdot 6H_2O$ (99.99%, Acros), $CuCl_2$ (99.9%, Aldrich), $InCl_3$ (99.99%, Aldrich), $HAuCl_4 \cdot 3H_2O$ (99.99%, Acros), $Fe(NO_3)_3 \cdot 9H_2O$ (98%, Aldrich), $AgNO_3$ (99.99%, Aldrich), $InCl_3$ (99.99%, Aldrich), and $PdCl_2$ (99.99%, Acros).

Typical synthesis of core–shell nanostrctures was as follows: 10 mL of 0.1 N ascorbic acid (vitamin C) was reacted with core $CuCl_2$ (2 mL, 0.1 N) at room temperature, and then shell $HAuCl_4 \cdot 3H_2O$ (2 mL, 0.01N) was added and allowed to react at room temperature for 1 h without using any capping or dispersing agents. Similarly, experiments were conducted using 0.01 N $Na_2PtCl_6 \cdot 6H_2O$, 0.01 N $PdCl_2$, 0.1 N $Fe(NO_3)_3 \cdot H_2O$, 0.1 N $InCl_3$ and 0.1 N $AgNO_3$ and the compositions are shown in Table 1. Control experiments were conducted using 2 mL of 0.01 N $Na_2PtCl_6 \cdot 6H_2O$, 0.01 N $PdCl_2$, 0.1 N Fe $(NO_3)_3 \cdot 9H_2O$, 0.1 N $InCl_3$, 0.1 N $AgNO_3$, and 0.01 N $HAuCl_4 \cdot 3H_2O$ with 10 mL of ascorbic acid. Transmission electron micrographs (TEM) were obtained from a JEOL JSM-1200 II microscope at an operating voltage of 120 kV. For TEM sample preparation, the solids were dispersed in water, and then a drop of dispersed particles was cast onto a copper grid and dried at room temperature.

Results and Discussion

The preparation of bimetallic nanoparticles from metal salts can be generally classified into two groups, that is, coreduction and successive reduction of two metal salts; the only difference is the number of metal precursors employed. Successive reduction is usually carried out to prepare core–shell structured bimetallic nanoparticles. Coreduction is the simplest preparative method of choice for bimetallic nanoparticles. In this process, first the metal ions coordinate to stabilize ascorbic acid, and then the reduction occurs. Addition of second metal salt and

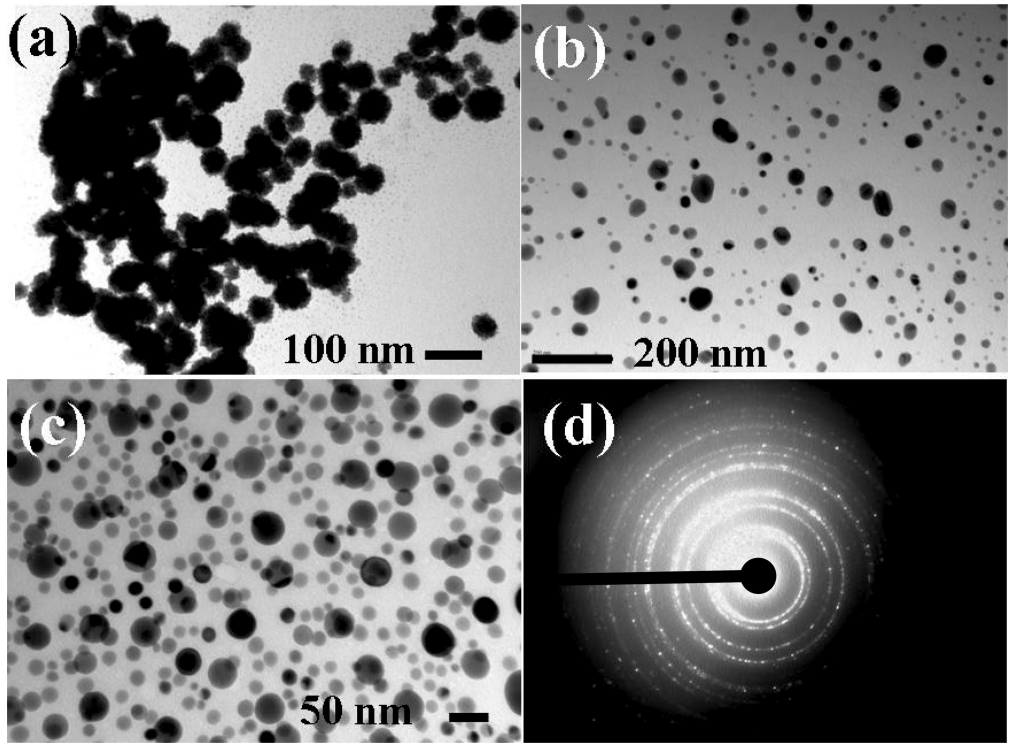

Figure 3. TEM images of core (Cu)-shell with (a) Pt, (b) Au, (c) Pd, and (d) selected area electron diffraction pattern of Cu-Pd core–shell nanoparticles.

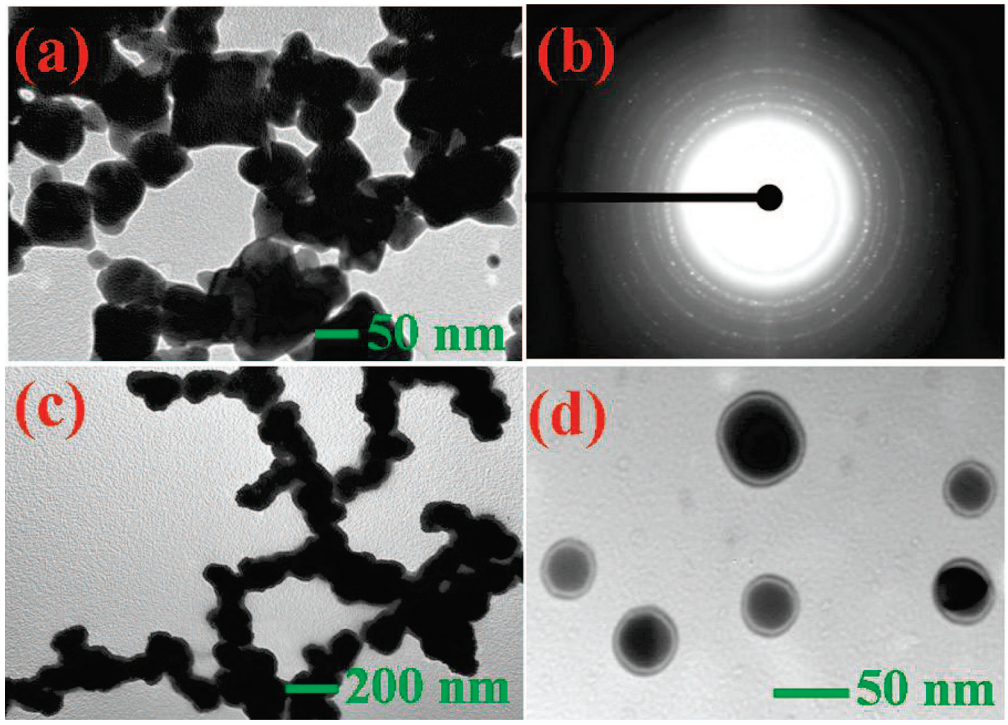

Figure 4. TEM images of core (Fe)-shell with (a) Au, (b) SAED of Au, (c) Pd, and (d) Pt core–shell bimetallic nanostructures.

subsequent reduction with excess stabilizing ascorbic acid results in the formation of the core–shell structure. The formation of core–shell structure will depend upon the metal salts used and the reducing/stabilizing agent used in the preparation. The schematic illustration of the core–shell formation is shown in Scheme 1.

Photographic images of the color formation of core–shell nanoparticles of Fe-Pd, Au-Pt, Pt-Fe, Au-Fe, Pd-Pt, and Au-Pd, reduced by ascorbic acid, are shown in Figure 1. The color formation drastically changed from control (see Figure 2) metallic reduction to core–shell formation (see Figure 1).

Platinum (shell) formed tennis ball kinds of structures on a Cu core (Figure 3), and Au-Cu and Pd-Cu formed regular spherical particles. The Pt-Cu core–shell nanoparticles were in the size range of 50–60 nm; Cu-Au and Cu-Pd core–shell nanoparticles were in the range of 5–50 nm. Selected area electron diffraction (SAED) patterns of Pd-Cu core–shell nanoparticles could be indexed to a cubic structure. Interesting

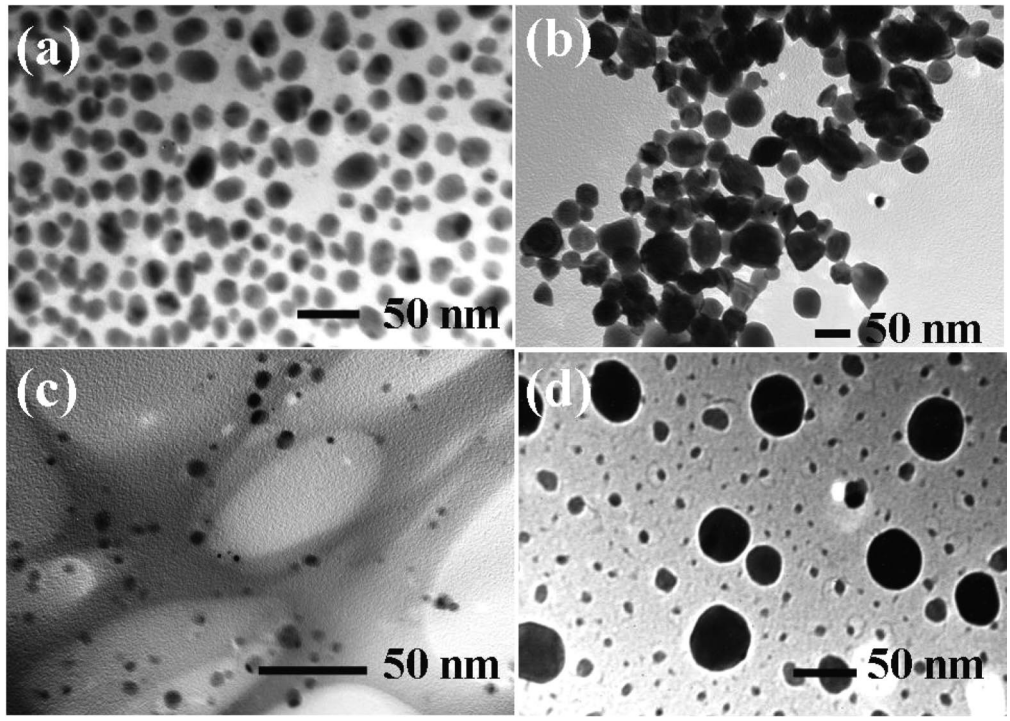

Figure 5. TEM images of metallic (control) noble nanoparticles synthesized using ascorbic acid (vitamin C) (a) Ag, (b) Pd, (c) Au, and (d) Pt.

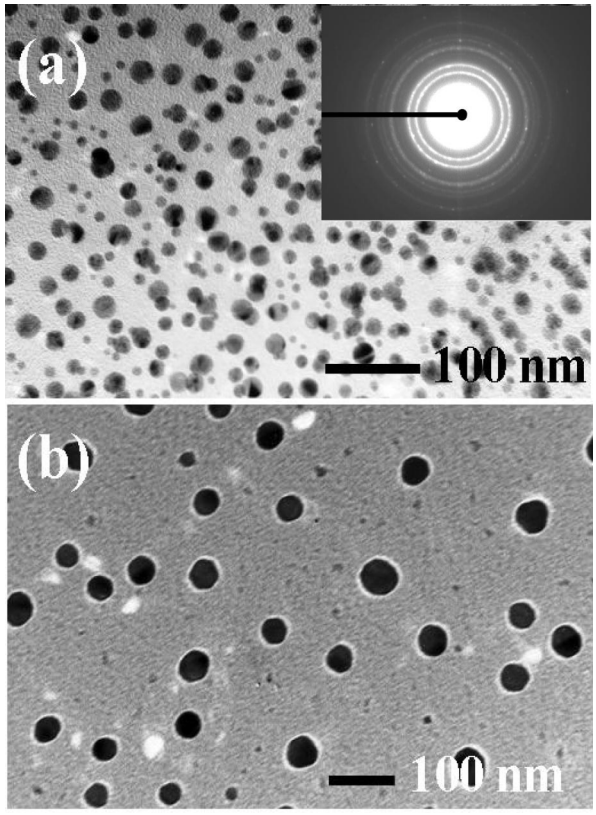

Figure 6. TEM images of metallic (control) noble nanoparticles synthesized using ascorbic acid (vitamin C) (a) Cu and (b) Fe. Inset shows corresponding SAED pattern image.

structures were obtained when Fe was used as the core and Au, Pd, and Pt were used as the shell material. The reduction of $Fe(NO_3)_3 \cdot 9H_2O$ with ascorbic acid yielded cube-shaped nanostructures, and concurrent addition of respective salts such as Au, Pd, and Pt provided a core–shell formation (Figure 4). However, in the case of the Pt-Fe core–shell, some spherical core–shell nanostructures were also observed along with cubic core–shell nanostructures. The control experiments with Au, Pt, Ag, Pd, Fe, and Cu resulted in spherical particles (Figures 5 and 6). The possible reason may be etching of the surface by the addition of other metallic salt as observed in the case of Pd by citric acid.[42] According to the wet etching model, chloride should play a role as a coordination ligand in the oxidative dissolution process. The major mechanistic question yet unanswered is how the addition of a small amount of noble metal chloride enabled the effective etching of Fe nanoparticles in aqueous media to make cubes. One possibility might be that the chloride ions could coordinate to Fe nuclei, thereby stabilizing them against aggregation, a primary mechanism for nanoparticle growth. Stabilization against aggregation could also sufficiently retard particle growth so that the back reaction, oxidative etching, would dominate and dissolution of surface would occur. Pending further mechanistic studies, the exact role of chloride in this synthesis remains elusive.

Chernov[43] and Xia et al.[44] have observed and modeled this type of growth as the basis for growth in dendrite and Pt systems. According to Xia et al.[44] the morphology of a particle evolves with two different conditions.[44] In the first condition, when the diffusion of an add-atom is very fast compared to the rate an add-atom is adsorbed onto the growing particle surface, the level of supersaturation is identical in regions very close to the particle's surface and far away from the particle. Any ridge that forms on the surface has a supersaturation level virtually identical to any other location on the growing crystal and is therefore not favored. The crystal will then grow into a shape that is dominated by the surface kinetics. Therefore, the

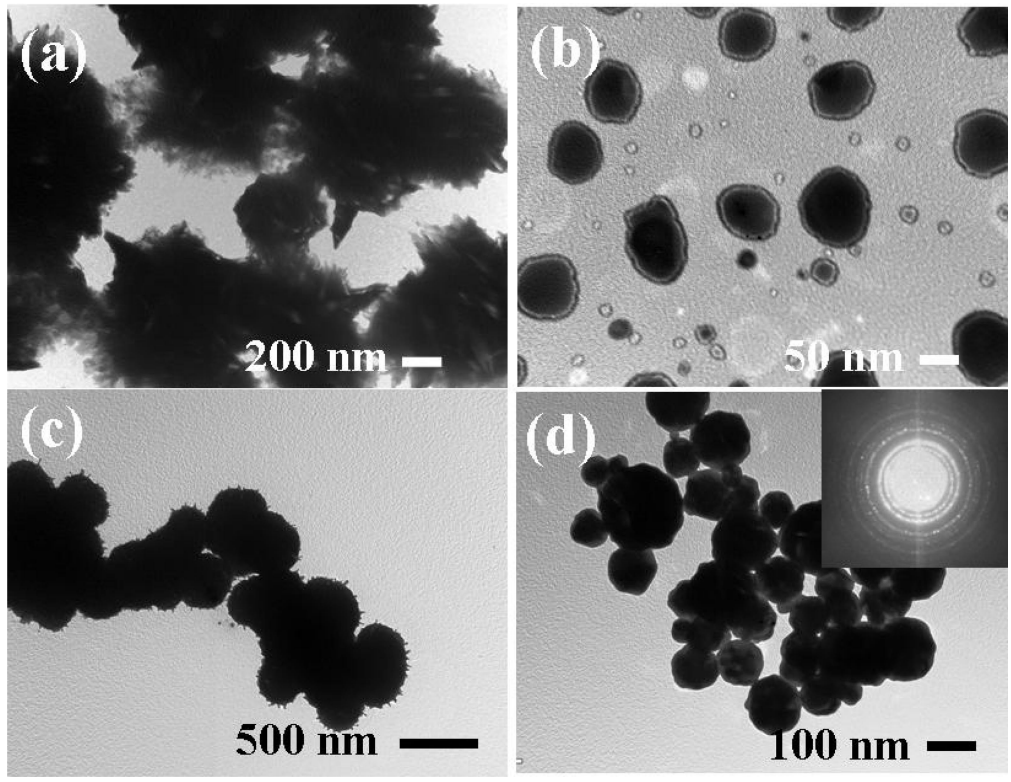

Figure 7. TEM images of Core (Pd)-shell with (a) In, (b) Pt, (c) Cu, and (d) Au core–shell bimetallic nanostructures.

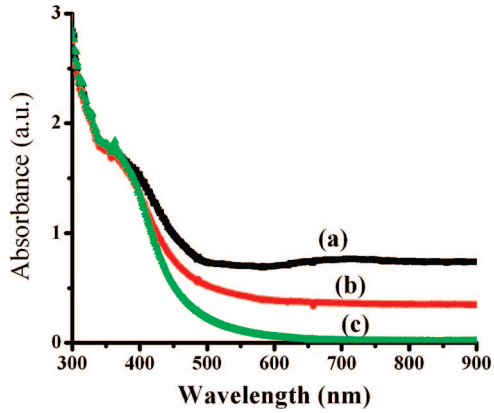

Figure 8. UV–visible spectra of core (Fe) shell with (a) Au, (b) Pd, and (c) Pt nanostructures synthesized using ascorbic acid.

crystal does not change its shape significantly over time as has been demonstrated using $NaNO_3$.[45]

In the second condition, the diffusion of an add-atom from solution to a growing crystal surface is slow compared to the rate a growth unit is adsorbed onto the particle surface. In this situation, a gradient occurs as the supersaturation at the particle surface is low and increases with distance from the particle. If a ridge forms on the particle's surface, it will have a slightly higher supersaturation at the top of the ridge than at the base. Then growth on the ridge will be encouraged by the supersaturation gradient. With a spherical particle under these conditions, any perturbation of the particle's surface will cause the particle's edges and corners to preferentially grow. Ridge growth should occur in directions directed by the particle's surface energies and may include curvature, step density, and crystalline anisotropy.

A similar situation arises[45] when $Fe(NO_3)_3 \cdot 9H_2O$ is reduced in the presence of other noble metal salts, wherein formation of $NaNO_3$ is favored in the case of $Na_2PtCl_6 \cdot 6H_2O$, HNO_3/HCl for $HAuCl_4 \cdot 3H_2O$, and chloride ions in the case of $PdCl_2$, respectively.

We have extended this strategy of making core–shell nanostructures to Pd metal as core particle with transition metals and other noble metals as shell structure. Pd with In forms brushlike needles (Figure 7a) on the core surface of the Pd. Pt-Pd core–shell nanostructures afforded (Figure 7b) similar kinds of structures as observed for Pt-Fe core–shell nanoparticles, but the shape of particle formation was spherical rather than cubes. In the case of Cu with Pd, sharp needles of Cu were formed on the surface of the Pd core (Figure 7c) and the Au-Pd system yielded regular spherical structures.

The UV spectra of the bimetallic nanoparticles were not a simple sum of the two monometallic nanoparticles, indicating that the bimetallic nanostructures have an alloy structure. Figure 8 shows the UV/vis spectra of these core (Fe) shell with (a) Au, (b) Pd, and (c) Pt nanostructures synthesized using ascorbic acid.

The absorption peaks that are typically found in the spectra of Pt, Pd, and Pt ionic precursors completely disappeared after reduction with ascorbic acid, showing the completion of reduction of both the ions. The core–shell nanoparticles had wider peaks than the starting mixture, showing that they had a less-ordered structure, which may suggest the formation of bimetallic bonds; that is Fe-Au, Fe-Pd and Fe-Pt nanostructures but may not unequivocally confirm core–shell structures.

The control UV–visible spectra of Au, Pt, Pd, Ag, Fe, and Cu are shown in Figures 9 and 10. The broad absorption peak

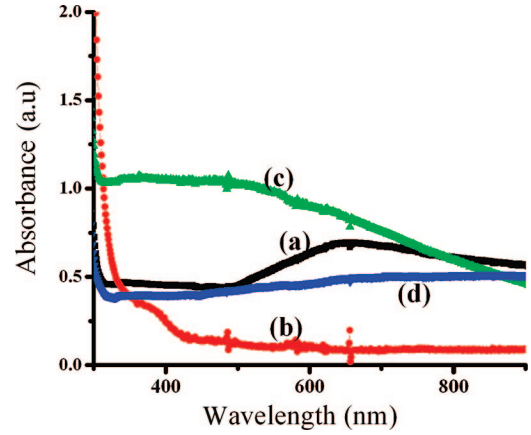

Figure 9. UV–visible spectra of control (a) Au, (b) Pt, (c) Pd, and (d) Ag nanostructures synthesized using ascorbic acid.

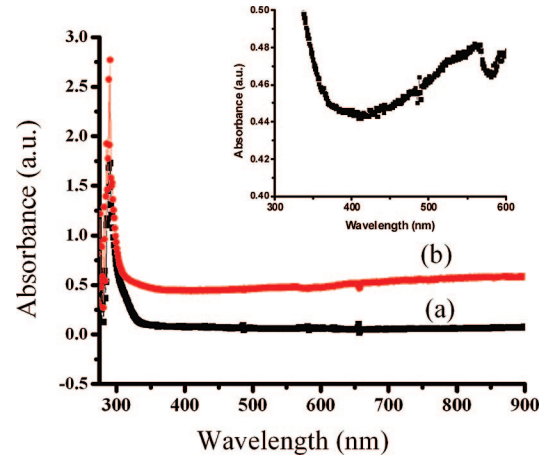

Figure 10. UV–visible spectra of control (a) Fe and (b) Cu nanostructures synthesized using ascorbic acid.

from 500 to 700 nm confirms the formation of Au nanoparticles (Figure 9a). Continuous absorption was observed of Pt and Pd in the visible region as expected (Figure 9b,c). Silver did show a broad plasma resonance peak in the 400 nm visible region. Particularly noteworthy are absorption peaks at 325 nm in the spectrum (Figure 10a) which can be used as an indicator for the formation of Fe (0). Copper nanoparticles were first produced by the ascorbic reduction of copper ions in aqueous solution, indicated by the appearance of plasmon resonance, with a significant contribution from interband transition which produces absorbance at around 500−700 nm (see inset Figure 10).

Conclusions

Nanostructures of core-(Fe, Cu)-shell (Au, Pt, Pd, and Ag) metals with varying shapes, such as cubes and spheres, with varying sizes can be synthesized using ascorbic acid (vitamin C) at room temperature without employing any capping or dispersing agents. The formation of core–shell structure depended on the core and shell material used for the preparation. Pt yielded tennis ball kinds of structures with a Cu core, whereas Pd and Au formed regular spherical nanoparticles. Au, Pt, and Pd formed cube-shaped structures with Fe as the core. The method can be extended to noble metals, such as Pd, as the core with transition metals, such as In and Cu, as the shell material wherein interesting structures such as brush and needle nanostructures were observed. This method is general, eco-

friendly, and occurred in a few seconds to afford different shapes and sizes; existing products may find useful roles in catalysis, biosensors, energy storage systems, nanodevices, and ever-expanding other technological applications.

Acknowledgment. M.N.N. was supported, in part, by the Postgraduate Research Program at the National Risk Management Research Laboratory administered by the Oak Ridge Institute for Science and Education through an interagency contract between U.S. Department of Energy and the U.S. Environmental Protection Agency.

References

(1) Agarwal, S.; Al-Abed, S. R.; Dionysiou, D. D. *Environ. Sci. Technol.* **2007**, *41*, 3722.
(2) Yen, C. H.; Shimizu, K.; Lin, Y.-Y.; Bailey, F.; Cheng, I. F.; Wai, C. M. *Energy Fuels* **2007**, *21*, 2268.
(3) Cwiertny, D. M.; Bransfield, S. J.; Roberts, A. L. *Environ. Sci. Technol.* **2007**, *41*, 3734.
(4) Pande, S.; Ghosh, S. K.; Praharaj, S.; Panigrahi, S.; Basu, S.; Jana, S.; Pal, A.; Tsukuda, T.; Pal, T. *J. Phys. Chem. C* **2007**, *111*, 10806.
(5) Link, S.; Wang, S. Z. L.; El-Sayed, M. A. *J. Phys. Chem. B* **1999**, *103*, 3529.
(6) Zafiropoulou, I.; Devlin, E.; Boukos, N.; Niarchos, D; Petridis, D.; Tzitzios, V. *Chem. Mater.* **2007**, *19*, 1898.
(7) Bao, Y.; Calderon, H.; Krishnan, K. M. *J. Phys. Chem. C* **2007**, *111*, 1941.
(8) Toshima, N.; Wang, Y. *Langmuir* **1994**, *10*, 4574.
(9) Yonezawa, T.; Toshima, N. *J. Chem. Soc. Faraday Trans.* **1995**, *91*, 4111.
(10) Freeman, R. G.; Hommer, M. B.; Grabar, K. C.; Jackson, M. A.; Natan, M. J. *J. Phys. Chem.* **1996**, *100*, 718.
(11) Ferrer, D.; Torres-Castro, A.; Gao, X.; Sepu'lveda-Guzma′n, S.; Ortiz-Me′ndez, U.; Jose'-Yacama'n, M. *Nano Lett.* **2007**, *7*, 1701.
(12) Liz-Marzán, L. M.; Philipse, A. P. *J. Phys. Chem.* **1995**, *99*, 15120.
(13) Esumi, K.; Shiratori, M.; Ishizuka, H.; Tano, T.; Torigoe, K.; Meguro, K. *Langmuir* **1991**, *7*, 457.
(14) Brust, M.; Walker, M.; Bethell, D.; Schiffrin, D. J.; Whyman, R. *J. Chem. Soc. Chem. Commun.* **1994**, 801.
(15) Mizukoshi, Y.; Okitsu, K.; Maeda, Y.; Yamamoto, T. A.; Oshima, R.; Nagata, Y. *J. Phys. Chem. B* **1997**, *101*, 7033.
(16) Remita, S.; Mostafavi, M.; Delcourt, M. O. *Radiat. Phys. Chem.* **1996**, *47*, 275.
(17) Sato, T.; Kuroda, S.; Takami, A.; Yonezawa, Y.; Hada, H. *Appl. Organomet. Chem.* **1991**, *5*, 261.
(18) Mulvaney, P.; Giersig, M.; Henglein, A. *J. Phys. Chem.* **1993**, *97*, 7061.
(19) Treguer, M.; de Cointet, C.; Remita, H.; Khatouri, J.; Mostafavi, M.; Amblard, J.; Belloni, J.; de Keyzer, R. *J. Phys. Chem. B* **1998**, *102*, 4310.
(20) Hodak, J. H.; Henglein, A.; Giersig, M.; Hartland, G. V. *J. Phys. Chem. B,* **2000**, *104*, 11708.
(21) Chen, Y. H.; Yeh, C. S. *Chem. Commun.* **2000**, 371.
(22) Slocik, J. M.; Naik, R. R. *Adv. Mater.* **2006**, *18*, 1988.
(23) Zhou, S.; Jackson, G. S.; Eichhorn, B. *Adv. Funct. Mater.* **2007**, DOI: 10.1002/adfm.200700216.
(24) Ketchie, W. C.; Murayama, M.; Davis, R. J. *J. Catal.* **2007**, *250*, 264.
(25) Inderwildi, O. R.; Jenkins, S. J.; King, D. A. *Surf. Sci.* **2007**, *601*, L103.
(26) Walsh, D.; Mann, S. *Nature* **1995**, *377*, 320.
(27) Correa-Duarte, L. M.; Giersig, M.; Liz-Marzan, L. M. *Chem. Phys. Lett.* **1998**, *286*, 497.
(28) Gittins, D. I.; Susha, A. S.; Wannemacher, R. *Adv. Mater.* **2002**, *14*, 508.
(29) Hu, J.; W.; Li, J.-F.; Ren, B.; Wu, D.-Y.; Sun, S.-G.; Tian, Z.-Q *J. Phys. Chem. C* **2007**, *111*, 1105.
(30) Pham, T.; Jackson, J. B.; Halas, N. J.; Lee, T. R. *Langmuir* **2002**, *18*, 4915.
(31) Pavan Kumar, G. V.; Shruthi, S.; Vibha, B.; Ashok Reddy; Kundu, T. K.; Narayan, C. *J. Phys. Chem.* **2007**, *111*, 4388.
(32) Cui, Y.; Ren, B.; Yao, J. L.; Gu, R. A.; Tian, Z. Q. *J. Phys. Chem. B* **2006**, *110*, 4002.
(33) Ah, C. S.; Hong, S. D.; Jang, D.-J. *J. Phys. Chem. B* **2001**, *105*, 7871.
(34) Tian, C.; Mao, B.; Wang, E. Kang, Z.; Song, Y.; Wang, C.; Li, S. *J. Phys. Chem. C* **2007**, *111*, 3651.
(35) Kobayashi, Y.; Salgueiriño-Maceira, V.; Liz-Marzán, L. M. *Chem. Mater.* **2001**, *13*, 1630.
(36) (a) Giersig, M.; Mulvancy, P. *Langmuir* **1996**, *12*, 4329. (b) Poastoriza-Santos, I.; Koktysh, D. S.; Mamedov, A. A.; Giersig, M.; Kotov, N. A.; Liz-Marzán, L. M. *Langmuir* **2000**, *16*, 2731.
(37) Ah, C. S.; Kim, S. J.; Jang, D.-J. *J. Phys. Chem. B* **2006**, *110*, 5486.
(38) Westcott, S. L.; Oldenburg, S. J.; Lee, T. R.; Halas, N. J. *Langmuir* **2000**, *16*, 6921.
(39) Nadagouda, N. M.; Varma, R. S. *Green Chem.* **2006**, *8*, 516.
(40) Nadagouda, N. M.; Varma, R. S. *Cryst. Growth Des.* **2007**, *7*, 686.
(41) Nadagouda, N. M.; Varma, R. S. *Macro. Rapid Commun.* **2007**, *28*, 465.
(42) Xiong, Y.; McLellan, J. M.; Yin, Y.; Xia, Y. *Angew. Chem., Int. Ed.* **2007**, *46*, 790.
(43) Herricks, T.; Chen, J.; Xia, Y. *Nano Lett.* **2004**, *4*, 2367.
(44) Chernov, A. *Sov. Phys. Crystallogr.* **1972**, *16*, 734.
(45) Lu, X.; Au, L.; McLellan, J.; Li, Z.-Y.; Marquez, M.; Xia, Y. *Nano Lett.* **2007**, *7*, 1764.

CG070554E